

***d*-band quantum well states in ultrathin silver films on V(100)**M. Kralj,<sup>1</sup> P. Pervan,<sup>1</sup> M. Milun,<sup>1</sup> T. Valla,<sup>2</sup> P. D. Johnson,<sup>2</sup> and D. P. Woodruff<sup>3</sup><sup>1</sup>*Institute of Physics, P.O. Box 304, 10000 Zagreb, Croatia*<sup>2</sup>*Physics Department, Brookhaven National Laboratory, Upton, New York 11973, USA*<sup>3</sup>*Physics Department, University of Warwick, Coventry CV4 7AL, United Kingdom*

(Received 20 May 2003; revised manuscript received 11 August 2003; published 15 December 2003)

We report an angle-resolved photoemission study of *d*-derived quantum well (QW) states in ultrathin silver films grown on V(100). Distinct *d*-derived QW states were observed for film thicknesses between 1 and 5 ML. Using a line shape analysis we conclude that for thicker films the *d* electrons are almost completely confined within the silver overlayer, suggesting a high reflectivity at the vanadium-silver interface. The energies of the QW states were found to be in good agreement with tight-binding calculations as well as with a phase accumulation model analysis. The calculations indicate a strong influence of the vanadium substrate on the energy of *d*-band QW states for the single-monolayer film.

DOI: 10.1103/PhysRevB.68.245413

PACS number(s): 79.60.Dp, 73.90.+f, 73.20.At, 79.60.Jv

**I. INTRODUCTION**

The properties of *d* bands in ultrathin metallic films have been the subject of experimental and theoretical research for a long time. Early experimental studies of the *d* bands in copper and palladium thin films deposited on a silver substrate by Eastman and Grobman<sup>1</sup> indicated a band narrowing effect. Theoretical calculations predicted a significant difference in the electronic structure with a reduction of the thickness.<sup>2</sup> However, detailed experimental characterization of the influence of reduced dimensionality on the *d* bands appears to require the use of very-high-energy resolution in order to resolve the numerous closely spaced *d* bands.

One of the first detailed angle-resolved photoemission spectroscopy (ARPES) studies of the Ag 4*d* bands in ultrathin films was reported by Tobin *et al.*<sup>3</sup> A silver film was deposited on a Cu(100) substrate, and due to the different binding energies of copper and silver bulk bands, the electrons in the silver 4*d* band were confined in the overlayer film, thereby showing two-dimensional (2D) behavior. It was later shown that an energetic offset of substrate and overlayer bands of the same symmetry can lead to the formation of stationary states in an overlayer, the so-called quantum well (QW) states.<sup>4</sup>

*s-p*-derived QW states in metallic films on metal substrates have been studied systematically in recent years, mostly by the use of ARPES.<sup>5,6</sup> On the other hand, similar quantization of the *d* bands due to localization in the overlayer films has attracted less attention due to the difficulty of resolving the numerous closely spaced *d* character QW states in a relatively narrow energy interval. Nevertheless, the existence of *d*-derived QW states has been clearly demonstrated for the Au/W(110) (Refs. 7 and 8), Ag/W(110) (Refs. 9 and 10), and Ag/Fe(100) (Ref. 11) systems.

In order for QW states to be observed in ultrathin noble-metal films deposited on a transition-metal surface, it is essential that there be a mismatch in energy of electron bands of the same symmetry in the substrate and overlayer film. This increases the reflectivity of the substrate interface for the electrons in the overlayer film. For this reason, the (100) surface of vanadium is particularly suitable for studying QW

states of *d* symmetry in silver films. The relative position of the silver *d* bands with the respect to those in vanadium is such that most of the Ag 4*d* bands fall into the symmetry band gap of the vanadium substrate projected on the (100) surface. At the  $\bar{\Gamma}$  point on the (100) vanadium surface the bottom of the  $\Delta_2$  band occurs at around 2.5 eV binding energy, well above the top of the Ag 4*d* band at 3.7 eV, making the relative shift of *d* bands in vanadium and silver as large as 1.2 eV. However, one should bear in mind that silver grows on V(100) in the form of fct rather than fcc, due to the lattice mismatch of 4%, so one can expect some differences in the electronic properties of silver films grown on the vanadium surface relative to the bulk form, although the size of this effect may not be very large. In presenting the results of recent calculations of the electronic structure of bulk fct silver with lattice parameters corresponding to the condition of epitaxial growth on V(100), Ernst *et al.*<sup>12</sup> concluded that the *d*-band dispersion was significantly larger than in fcc Ag, leading to an increase of the silver *d*-band width. Indeed, their results show the top of the band extending up to 2.5 eV below the Fermi level, which might imply that the *d*-derived QW states in silver films on V(100) should exist over a much wider energy range than is observed for Fe(100) and W(110) substrates where the silver grows without any significant mismatch with respect to its bulk value. However, the fact that compared to bulk silver the top of the band is closer to the Fermi level in these calculations appears to be a consequence of an overall energy shift of the band, rather than being due to a large increase in the width. Such a shift is also seen in calculations of the band structure of fcc Ag based on the local density approximation, and while the band dispersion appears to be consistent with experiment, an offset of the band energies relative to experiment appears to be a systematic feature of the method.<sup>13</sup>

In the present study of epitaxially grown silver films on V(100), we concentrate on film thicknesses ranging between 1 and 5 ML (monolayers), for which we can prepare well-ordered films with distinct photoemission features. Previous studies of the Ag/V(100) overlayer system have characterized in detail the silver growth mode in the low-coverage limit. It has been shown that up to 2 ML, silver grows

pseudomorphically on a V(100) surface<sup>14</sup> in an extremely well-ordered fashion, producing layers with a low defect density and with an unmatched spectral intensity of the *s-p*-derived QW states.<sup>15</sup> The latter observation is regarded as a clear indication of the high quality of the overlayer films.<sup>16</sup> Around room temperature further growth remains layer by layer, while above room temperature, all silver in excess of the 2 ML layer film condenses to 3D clusters. Note that these earlier studies showed that the energies of the *s-p* QW states observed in photoemission provided an excellent calibration of the film thickness and homogeneity; films with fractional monolayer coverages showed the coexistence of *s-p* QW states characteristic of the individual component integral monolayer films,<sup>15</sup> and as we will show, the same effect is seen in the photoemission spectra from the *d*-band QW states.

The experiments reported here were carried out at the National Synchrotron Light Source (NSLS) of Brookhaven National Laboratory (BNL) using undulator beamline U13UB, which provides photon energies in the range between 12 and 23 eV, and at the VUV beamline at the ELETTRA synchrotron in Trieste. At the latter beamline it was possible to work over the much wider photon energy range of 18–100 eV. At both stations, the light was *p* polarized and incident on the sample at an angle of 45°. The electron energy analyzer at BNL was a Scienta SES-200, which collects simultaneously photoelectrons at a range of energies (about 2 eV) and angles ( $\approx 12^\circ$ ). The combined instrumental energy resolution could be set to a value in the range 8–25 meV. The angular resolution was  $\approx 0.2^\circ$ . The electron energy analyzer at Elettra was a VSW-50 with a resolution of around 30 meV. Monolayer films were prepared by depositing silver onto the surface at a substrate temperature of 60 K, followed by brief rapid heating to 900 K. This procedure usually produced a monolayer film with a very low concentration of defects. Thicker films, up to 5 ML, were prepared by subsequent low-temperature silver deposition onto a well-ordered 1 ML film, followed by annealing to room temperature.

## II. RESULTS

### A. ARUPS of *d*-band quantum well states

Figure 1 shows normal emission spectra recorded at a photon energy of 24 eV from 1 and 2 ML silver films deposited on V(100). The peaks at 1.7 and 0.6 eV below the Fermi level correspond to photoemission from QW states of *s-p* symmetry. The energy dependence of the photoemission intensity from *s-p* QW states in silver films on vanadium (100) is well documented.<sup>15</sup> The spectral intensity in the range of energies more than 4 eV below the Fermi level corresponds to photoemission from QW states of *d* symmetry. The anticipated number of *d*-band QW states increases with film thickness as  $5N$  (where  $N$  is the number of silver atomic layers) for each spin state, but the broadening of the peaks induced by Coster-Kronig Auger processes makes the process of resolving all the QW states difficult and potentially unreliable, even for the very thinnest film. By comparison with photoemission spectra taken over an extensive range of photon

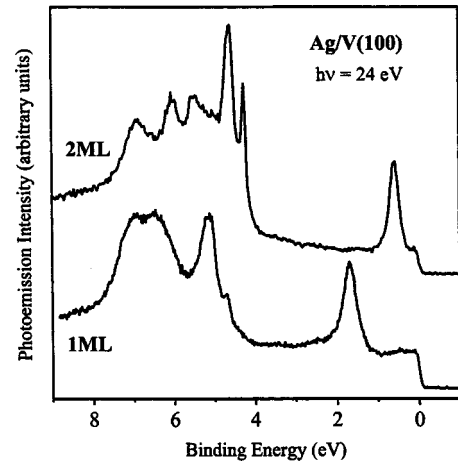


FIG. 1. Normal-emission photoelectron energy spectra recorded at a photon energy of 24 eV from 1 and 2 ML Ag films deposited on V(100).

energies, it is possible to identify four peaks in the 1 ML film which we have labeled  $P_1$ – $P_4$  in Fig. 2(a) (notice, though, that peak  $P_2$  clearly has at least two distinct components when recorded at higher spectral resolution—see Figs. 3 and 4). The binding energies associated with these peaks exhib-

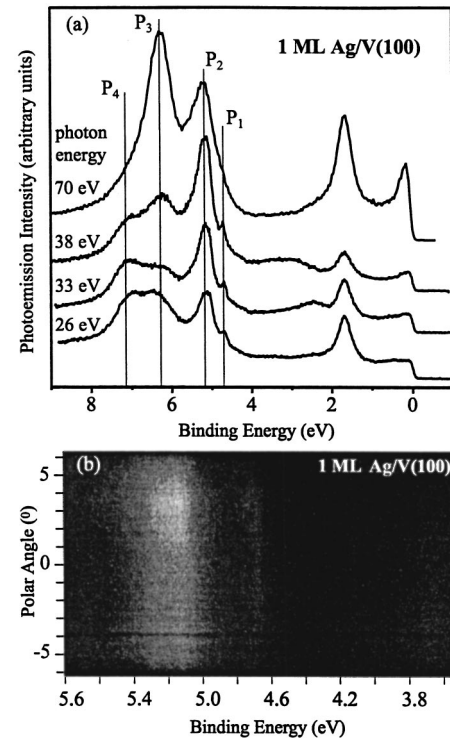


FIG. 2. (a) Normal-emission photoelectron energy spectra recorded at different photon energies from 1 ML Ag film. (b) Photoemission intensity map as a function of initial-state electron binding energy and polar emission angle (proportional to the component of the electron momentum parallel to the surface) from a 1 ML film of Ag on V(100) recorded at a photon energy of 18 eV. The two bright lines correspond to emission from the  $P_1$  and  $P_2$  states and clearly show no significant dispersion in parallel momentum around normal emission (corresponding to the center of the Brillouin zone).

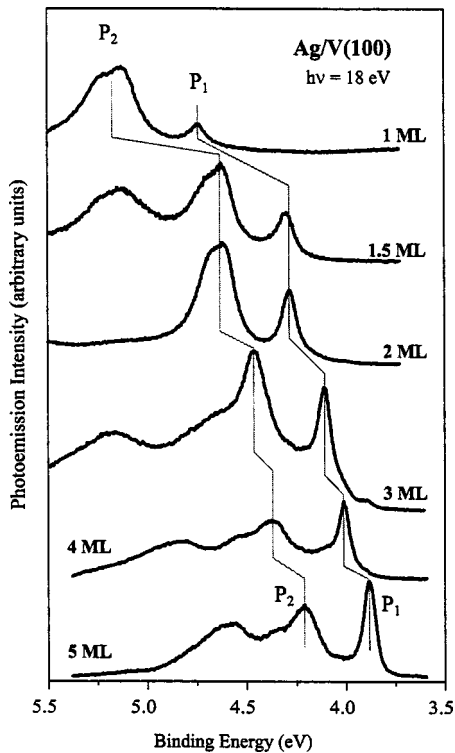


FIG. 3. Normal-emission photoelectron energy spectra showing the  $d$ -band QW peaks recorded at a photon energy of 18 eV from Ag films of different thicknesses on V(100). Notice that the spectrum from the 1.5 ML films shows the peaks characteristic of the 1 and 2 ML films from which it must be composed.

ited no dependence of peak position on photon energy. Of course, even the  $d$  bands of bulk solids are relatively flat, but the complete absence of dispersion in  $k_{\perp}$  seen in these  $d$ -band QW states would appear to be a consequence of their spatial localization within the ultrathin Ag film; we return to this point in Sec. III A below. Figure 2(b) shows raw data from the position-sensitive detector of the Scienta analyzer which provides a photoemission intensity map as a function of energy and polar emission angle (proportional to the electron momentum parallel to the surface) recorded at a photon energy of 18 eV; the two bright lines correspond to emission from the  $P_1$  and  $P_2$  bands and show no significant dispersion in parallel momentum of either state. However, more careful analysis of the energy distribution curves (EDC's) of the  $P_1$  band, recorded at different emission angles, does reveal a slight negative dispersion with parallel momentum.

Analysis of the photoemission spectra from  $d$ -band QW states in the 2 ML film is already significantly more difficult than for the 1 ML film. Two QW states should now be derived from each  $d$  band. Determining the identity of a particular peak can be rather difficult, and sometimes the evidence is conflicting. For this reason we have restricted our analysis of QW states in the thicker films to a small number of states in the reduced binding energy range from 3.5 to 5.5 eV. This energy range includes peaks  $P_1$  and  $P_2$  where the leading peak ( $P_1$ ) is not affected by lifetime broadening due to Auger decay and consequently is the narrowest state in the  $d$ -band manifold. Figure 3 shows a set of the normal emis-

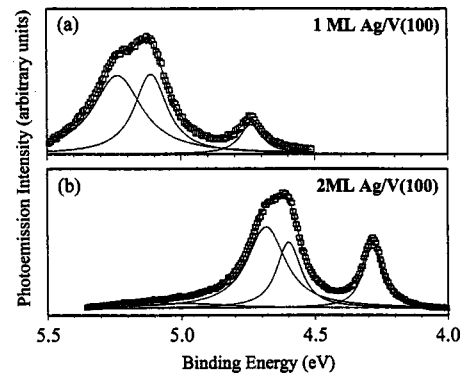


FIG. 4. (a) Normal-emission photoelectron energy spectra in the energy range of the  $P_1$  and  $P_2$   $d$ -band QW peaks recorded from a 1 ML Ag film deposited on V(100). The fit and associated individual components obtained from a line shape analysis are shown as solid lines. (b) The same for a 2 ML Ag film showing a decrease of the  $P_2$  peak splitting.

sion spectra recorded from 1–5 ML silver films. These spectra were taken with the higher-energy-resolution spectrometer (Scienta SES-200 at BNL), enabling us to observe additional structure not seen in the spectra of Figs. 1 and 2(a) (recorded at Elettra); notice, in particular, the clear splitting of peak  $P_2$  from the 1 ML film. The spectra exhibit a pattern typical of QW states: a shift to smaller binding energy with increasing film thickness.<sup>17</sup> Peak  $P_1$  shifts from 4.75 eV (1 ML) to 3.85 eV (5 ML) with respect to the Fermi level. A shift of the same order (0.9 eV) is also seen for the  $P_2$  state for the same thickness range. A large fraction (0.55 eV) of this total shift in going from 1 to 5 ML is associated with the increase of the film thickness from 1 to 2 ML. The leading  $P_1$  peak is well separated from the other photoemission peaks, which makes its line shape analysis more reliable. For all film thicknesses this peak could be fitted with a Lorentzian lineshape (e.g., Fig. 4). The peak width increases from 61 to 95 meV as the film thickness reduces from 5 to 1 ML. For some particularly uniform 2 ML films the Lorentzian width of the  $P_1$  peak was found to be 65 meV. Peak  $P_2$  clearly shows a splitting, which reduces with increasing film thickness: 120 meV for 1 ML and 80 meV for 2 ML spectra (see Fig. 4). No splitting of this peak could be resolved in the spectra from films of 3 ML or more, although for the thicker silver films the peak is broader.

Notice, incidentally, that for the thicker films there is almost certainly some slight nonuniformity in the thickness, leading to weak additional structure. For example, the weak but distinct peak seen in the spectrum from the 3 ML film at a binding energy of 3.9 eV is probably due to the  $P_1$  peak from small areas of 5 ML coverage, while small areas of 4 ML may give rise to the high-energy “tail” of the  $P_1$  peak in the 3 ML spectrum. Indeed, as remarked earlier, the  $d$ -band QW peaks observed provide a valuable monitor of the film thickness and homogeneity. The spectrum included in Fig. 3 for a nominal film thickness of 1.5 ML illustrates this rather clearly. At 1.5 ML average thickness half the surface must be covered with 1 ML and the other half with 2 ML, so the photoemission spectrum shows the  $d$ -band QW peaks associated with these two film thicknesses.

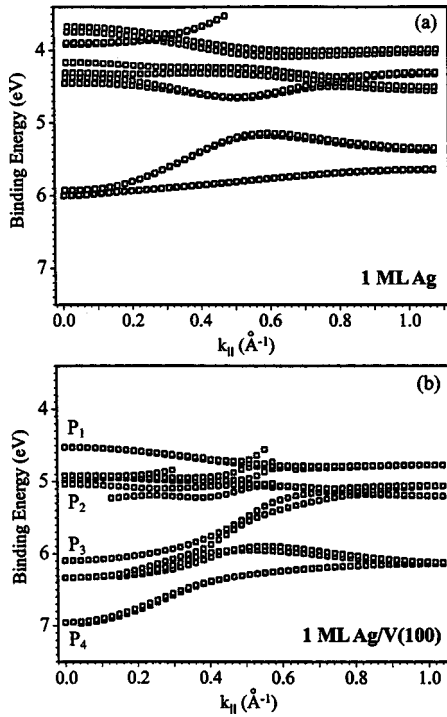


FIG. 5. (a) Calculated tight-binding band structure of an unsupported silver monolayer along the  $\langle 110 \rangle$  direction. (b) Calculated tight-binding band structure of a silver monolayer on V(100) the  $\langle 100 \rangle$  direction of the substrate (corresponding to the same  $\langle 110 \rangle$  direction of the Ag overlayer). Only states with more than 30% weight in the surface layer are shown.

### B. Tight-binding calculation

In order to model the Ag/V(100) system and to determine the influence of the vanadium substrate on the silver  $d$ -band QW states we have performed tight-binding calculations. The calculations, described in more detail elsewhere,<sup>18</sup> are implemented in the slab format with each layer having a basis of 18 states, 9 ( $5d$ ,  $3p$ , and  $1s$ ) for each spin. The calculation has been modified to include the spin-orbit interaction using the standard Hamiltonian to describe the  $d$  blocks:<sup>19</sup>

$$H = \begin{vmatrix} H_{dd} + \xi M & \xi N \\ -\xi N^* & H_{dd} + \xi M^* \end{vmatrix}. \quad (1)$$

Here spin-orbit splitting effects are included through the matrices  $M$  and  $N$  and the spin-orbit parameter  $\xi$ . Values for the latter are taken from the compilations of Herman and Skillman.<sup>20</sup>

Figure 5(a) shows the calculated tight-binding (TB) silver band structure in the energy range of the  $d$  bands (the calculations also include, of course, the  $s$ - $p$  bands) for an unsupported monolayer along a  $\langle 110 \rangle$  direction while in Fig. 5(b) the same band structure is shown for a silver monolayer deposited on V(100). In the latter case we show only bands with more than 30% of their weight in the surface layer. Because Ag is fcc and V is bcc and because the symmetry is defined with respect to the substrate, the direction  $\langle 110 \rangle$  for the unsupported silver monolayer corresponds to a  $\langle 100 \rangle$  di-

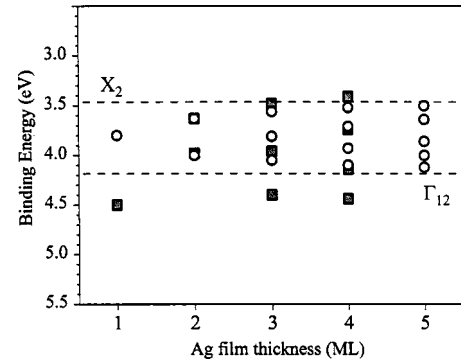


FIG. 6. Calculated energies of the  $d_{xy}$ -symmetry QW states (corresponding to the  $P_1$  photoemission peak) for unsupported silver layers (open circles) and the silver layers in contact with vanadium (100) surface (solid squares) as a function of film thickness.

rection of the vanadium. The calculated energies at the center of the Brillouin zone,  $\bar{\Gamma}$ , are such as to suggest that the experimental peaks  $P_1$ – $P_4$  (Fig. 2) can be assigned to these bands as labeled in Fig. 5(b). There are several features that characterize the vanadium influence on the band structure of a silver monolayer. There is an overall and significant reduction of the electron binding energy when the silver monolayer is put in contact with the vanadium surface. In addition, comparisons with the results of calculations which neglect the effects of spin show that the effects of the spin-orbit splitting are significantly reduced by interaction with the V substrate. Notice that although the experimental results show that the energies of peaks  $P_1$  and  $P_2$  appear to move in tandem with increasing film thickness (Fig. 3) and have a separation approximately equal to that observed for the spin-orbit interaction in atomic silver, the calculations show clearly that they do not represent a spin-orbit split doublet.

On the basis of our tight-binding calculations we make the following symmetry assignments for the bands  $P_1$ – $P_4$ :  $P_1$  has  $d_{xy}$  character, and  $P_2$  is a mix of  $d_{xz}$  and  $d_{yz}$ .  $P_3$  is of  $d_{z^2}$  and  $d_{x^2-y^2}$  character while  $P_4$  seems to be predominantly  $s$ - $d_{z^2}$  with the strongest hybridization to the bulk. Notice that the topmost band  $P_1$  shows only slight negative dispersion with parallel electron momentum, while  $P_2$  is almost constant in energy around the center of the zone, consistent with the results for the 1 ML silver film shown in Fig. 2(b) and described in the previous section. The symmetry of silver bands associated with the  $P_1$  and  $P_2$  peaks is such that no significant hybridization is expected with the even-symmetry vanadium band in the observed energy range.

Figure 6 shows the dependence of the calculated binding energies of the  $d_{xy}$  QW states (associated with the  $P_1$  peak) in the silver film as a function of film thickness. Open circles correspond to the QW states for an unsupported silver film, while solid squares represent the energies of QW states in silver films on V(100). As expected, for unsupported silver films, the QW states for the thicker films appear symmetrically at higher and lower binding energies around the 1 ML state. Experimentally, the systems that show behavior most like this are physisorbed Xe multilayers,<sup>21</sup> for which the interaction with the substrate is negligible. The strongest influ-

ence of the vanadium substrate on the silver  $d_{xy}$  QW state is, not surprisingly, for the 1 ML film. This state is pulled down in energy by 750 meV. More surprising, perhaps, is that within this model the effect of the substrate on the mean energy of the QW states decays rapidly with film thickness.

### III. DISCUSSION

#### A. Silver-vanadium interface

There are several factors that suggest that the  $4d$  electrons in the silver films are well confined within the film, despite the fact that barrier at the vanadium-silver interface is not an absolute band gap, but rather an energy offset of states of the same symmetry in the substrate and overlayer. One indication of this is the complete lack of dispersion of the QW state energies with the component of the electron momentum perpendicular to the surface (explored experimentally by varying the photon energy and thus the final state photoelectron momentum); if the states in the Ag film coupled to extended substrate bands, some degree of dispersion might be expected. Of course, in the case of  $d$  states, even the bulk bands are relatively flat. However, we have previously shown that this same absence of dispersion is seen for the  $s$ - $p$ -derived QW states in this Ag/V(100) system which show no photon energy dependence of their binding energies even in thicker silver films (8 ML).<sup>15</sup> The present observations indicate that the  $d$ -band QW states show the same high degree of localization.

We should also note that even in the absence of an energy or symmetry gap at the substrate/film interface, which must result in incomplete confinement of the electrons in the overlayer film, well-defined QW resonances can still be formed if the interaction across the interface is not too strong. A valuable analog for describing this situation is the optical Fabry-Perot interferometer model, in which the incomplete confinement can be regarded as a partial reflectivity at the substrate/film interface.<sup>22</sup> A partial reflectivity leads to an energy broadening of the QW resonances. Such broadening, in addition to the lifetime broadening induced by photohole interactions with electron and phonon excitations or scattering at impurities, has been reported for  $d$ -band QW states in silver on Fe(100).<sup>11</sup>

Our analysis of the width of the photoemission peaks from the  $P_1$   $d$ -band quantum well state (see Fig. 3) indicates that the effective reflectivity at the Ag/V(100) interface may well be different from that reported for the Ag/Fe(100) interface. Figure 7 shows the Lorentzian width of the  $d$ -band QW states closest to the Fermi level for Ag films on V(100), Mo(110) (Ref. 23) and Fe(100). The peak widths for Ag on Mo and V are the Lorentzian widths of the experimental spectra while the widths shown for Ag on Fe are Lorentzian widths with an additional correction for the instrumental broadening. The solid curve [calculated from Eq. (3) of Ref. 11] is a fit to the Ag/Fe(100) data assuming a value for the reflectivity of  $R=0.68$  and a lifetime broadening  $\Gamma = 13$  meV, the values found by Luh *et al.*<sup>11</sup> Clearly, the peak widths of the QW states in the thinner silver films on vanadium and molybdenum are substantially smaller than those predicted for the same silver film thicknesses on an iron sub-

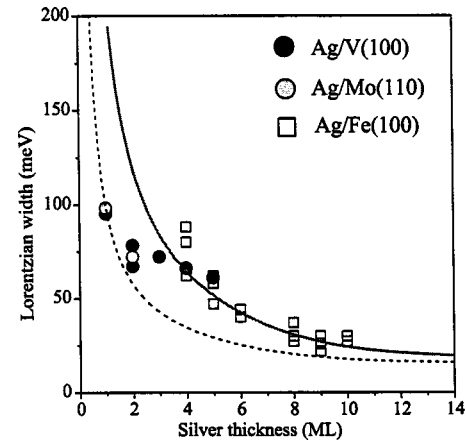


FIG. 7. Lorentzian peak width of the  $P_1$  photoemission  $d$ -band QW peak as a function of silver film thickness on several different substrates. The data for Ag/Fe(100) (solid diamonds) and Ag/Mo(110) (solid circles) are taken from Refs. 11 and 23, respectively. The solid curve is calculated using Eq. (3) of Ref. 11 using the same parameters found to give a good fit to the Ag/Fe(100) data ( $\Gamma = 13$  meV,  $R=0.68$ ). The dashed curve uses a larger value of the reflectivity ( $R=0.85$ ).

strate on the basis of this curve. While the complete set of experimental data points from the three different substrate appears to fall on a reasonably smooth curve in Fig. 7, no single set of values of  $\Gamma$  and  $R$  fits all of these points. For example, the dashed curve in Fig. 7 shows the effect of increasing  $R$  to 0.85, providing an excellent fit to the data point corresponding to 1 ML of Ag on V(100), but clearly not fitting the other points. If the lifetime broadening  $\Gamma$  is increased from its very low value of 13 meV, even higher  $R$  values are required to fit this point. Notice, incidentally, that one further parameter needed to generate these curves is the group velocity of the electrons in the various QW states, but this can be estimated from the curvature of the relevant Ag bulk  $d$  band. It is perhaps not surprising that no single set of  $\Gamma$  and  $R$  values fits all these data, as they correspond to different binding energies and thus to different locations in the symmetry barrier presented at the film/substrate interface. In this regard, we may note that all the Ag/Fe(100) data points (which are fitted well by a single pair of parameter values) do correspond to states in a very narrow energy range.

Of course, if different  $\Gamma$  and  $R$  values are expected for the different experimental points for the Ag/V(100) system, there is no longer a unique solution which fits the observed spectral width. In this regard, the comparison with the data from the Mo(110) substrate are helpful. In the case of silver films grown on Mo(110), the  $P_1$  QW state falls within a total band gap that exists in the range from 5.0 to 3.7 eV below the Fermi level. It is therefore reasonable to assume that within this energy range the reflectivity is complete, and we may use the widths measured for films grown on the molybdenum substrate as a gauge of the reflectivity at the vanadium substrate. The fact that the widths of the QW photoemission peaks in films grown on the two substrates are identical leads us to the conclusion that the reflectivity at the vanadium

surface is similar to that at the molybdenum surface, further reinforcing the view that  $R$  is close to unity for our Ag/V(100) system. This implies that the symmetry gap of the vanadium surface is as efficient a barrier as the total energy gap of molybdenum.

### B. Silver monolayer

As a special case, we now discuss the case of a single monolayer film. For the 1 ML film low-energy electron diffraction<sup>14,24</sup> (LEED) and scanning tunneling microscopy<sup>25</sup> (STM) measurements have shown that silver atoms adopt the periodicity of the underlying vanadium surface despite the 4% lattice mismatch between the bulk (100) silver fcc and vanadium bcc planes. Figure 2(a) shows that the upper- and lower-lying  $d$  bands in the center of the Brillouin zone have energies of 4.7 and 6.25 eV, respectively. This makes the width of the  $d$  band in the single-monolayer film equal to 2.4 eV, a substantial reduction from the 3.8 eV characteristic of the bulk silver  $d$  band.

The results of our tight-binding calculations for an unsupported and an adsorbed silver monolayer indicate a strong influence of the vanadium substrate on the Ag  $4d$  electron bands. The energy of these bands is reduced through interaction with the vanadium substrate by an average of 0.75 eV while the total  $d$ -band width remains virtually unchanged. The agreement between the peak positions of the experimentally measured normal-emission spectra recorded from the monolayer film [see Fig. 2(a)] and the calculated energies in the center of the Brillouin zone is surprisingly good. Apart from a rigid offset of 200 meV, the calculated energies correspond to the measured ones. The tight-binding calculation also gives an indication of the spin-orbit interaction. For the silver monolayer on a vanadium surface the spin-orbit interaction induces a splitting of the  $P_2$  band in the center of the zone. The combined action of spin orbit interaction and crystal field induces an energy band splitting of around 0.12 meV, which is the same value as that obtained from the experimental spectral analysis shown in Fig. 4. The spin-orbit splitting in the isolated atom is 0.224 eV, and this same value has been reported for 1 ML Ag/Cu(100) where the interaction of the silver overlayer with copper substrate is expected to be weak.<sup>3</sup>

As Fig. 2(a) shows, the intensities of the  $d$ -band QW photoemission peaks are dependent on the photon energy. The observed photon energy dependence appears quite different from that of the  $s$ - $p$  QW states in this system<sup>15</sup> in that there are no intensity oscillations of the photoemission peaks. Generally, peaks  $P_2$  and  $P_3$  increase in intensity with photon energy. The intensity of the  $P_1$  peak is weak for all photon energies; this peak is associated with a formally forbidden transition from a state of  $d_{xy}$  symmetry.

### C. Phase accumulation model analysis

The phase accumulation model is a simple way of predicting the energy of QW states. In this model the condition for a stationary state is determined by summing the phase accumulated by an electron making a round trip within the overlayer film and requiring that this is an integral multiple of

$2\pi$ . Despite its inherent simplicity and somewhat crude approximations, the phase accumulation model has been used with considerable success to describe the system and thickness dependence in ultrathin films of the energies of quantum well states and resonances  $s$ - $p$  (Refs. 26–30) and  $d$  (Refs. 8, 9, and 11) symmetries. The phase accumulation equation has the form

$$\phi_C(E) + \phi_B(E) + 2k(E)d = 2\pi n, \quad (2)$$

where  $k$  is the electron wave vector,  $n$  an integer, and  $\phi_C(E)$  and  $\phi_B(E)$  are the phase shifts associated with the reflections at the substrate/film and film/vacuum interfaces, respectively.<sup>31</sup> We have used the standard function to describe the energy dependence of the phase shift  $\phi_B(E)$  at the vacuum side of the film based on an image-potential barrier.<sup>26</sup> In the absence a well-defined hybridization gap (which occurs for the  $s$ - $p$  QW states in this system) the proper choice of  $\phi_C(E)$  is less clear. We therefore chose the simplest possible assumption of setting the phase change at this interface to a constant value. We find that a value for  $\phi_C(E)$  of  $0.21\pi$  gives a reasonable description of the experimental (and theoretical tight-binding) results. With a fixed value for  $\phi_C(E)$  the change in the total phase is derived entirely from the film thickness and the vacuum barrier. Notice, incidentally, that for states well below the vacuum level (as is the case for occupied QW states) the phase shift  $\phi_B(E)$  is also almost constant over the energy range of interest to us here. While a free electron description of the energy dependence of the wave vector is a natural choice to describe  $s$ - $p$  QW states, this is much less obviously appropriate to describe  $d$ -band QW states. Parametrized functions have been used in the literature to describe  $k(E)$  for these cases.<sup>10,11</sup> We have found that the parametrized function, generated from a simple linear chain model,<sup>8,10</sup> reproduces the silver  $4d$  energy bands satisfactorily. This parametrization defines the dispersion between the upper and lower energies of each band, and these values are taken from Ref. 11.

Figure 8 shows a graphical solution of Eq. (2). The bold lines, almost parallel to the abscissa, show the term  $[\phi_C(E) + \phi_B(E) - 2\pi n]$  while the thinner solid and dotted lines show  $-2kma$  where the layer spacing is given by  $a$  and the number of layers is  $m$ . The crossing points correspond to predicted QW binding energies. In order to account for the energy of the QW states,  $P_1$  and  $P_2$ , we have generated three sets of  $k(E)$  functions which are generated from three highest-energy bulk silver  $4d$  bands [ $\Delta(7)$ ,  $\Delta(7)$ , and  $\Delta(6)$ ]. The related curves in Fig. 8 are fine dotted, thin solid and coarse dotted lines, respectively. To simplify comparison with the photoemission data in Fig. 3 we have marked in Fig. 8 only the highest-energy solutions for each branch of  $k(E)$  and for each silver film thickness in the range from 1 to 5 ML. Notice, incidentally, that all the solutions marked correspond to the condition  $m = n + 1$ , so for each film thickness the solutions fall on the same bold line which actually corresponds to a fixed value of  $n$ . We see that most of the trends observed experimentally are reproduced by the phase accumulation model. The solid squares reproduce reasonably accurately the shift of the  $P_1$  QW state to smaller binding

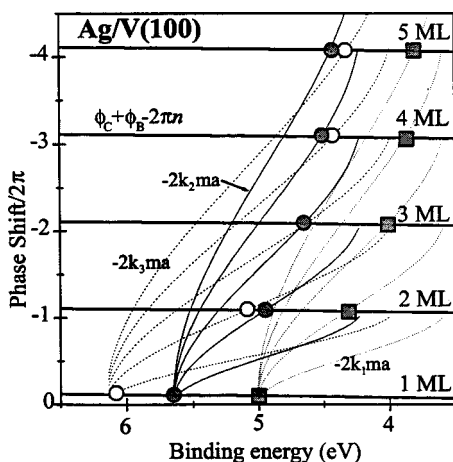


FIG. 8. Graphical solution of the phase accumulation model equation (2) for  $d$ -band QW states in silver films on V(100). The fine dotted, thin solid, and coarse dotted lines represent the phase change associated with electron propagation within the well in the different silver bulk bands  $k(E)$  for different film thickness ( $m$  ML). The solid bold curves represent the sum of the phase change at the vacuum and the interface barriers plus an integral number of factors of  $2\pi$ . Notice that for each silver film thickness only the highest-energy solutions are marked (open and solid circles and solid squares). See the text for fuller details.

energies with increasing film thickness including the effect we have already remarked upon of a particularly large decrease of binding energy between the 1 and 2 ML films. Both the solid and open circles can be associated with the observed  $P_2$  peak, which is observed to have a splitting which decreases with the film thickness such that it is no longer observed for a film thickness of 3 ML. The phase accumulation model predicts that for thicknesses greater than 3 ML the  $P_2$  peak splitting should increase again. However, due to the increasing number of states generated for each new silver layer and the increasing width of the peaks, it is no longer possible to observe this splitting experimentally.

Although no data for films thicker than 5 ML are available, the thickness dependence of the energy of the leading peak  $P_1$  (see Figs. 3 and 8) indicates that with increasing thickness, the highest energy this branch of the QW states would reach is approximately 3.5 eV below the Fermi level.

This should correspond to the top of the  $d$  bands of the bulk overlayer and is about 1 eV lower than that calculated for bulk fct silver;<sup>12</sup> we have already noted, however, that this discrepancy may be due to an offset of the calculated  $d$  bands which appears to be characteristic of such calculations.<sup>13</sup> It is interesting to note that the energies of the leading  $d$ -band QW states in the 4- and 5-ML-thick silver films on Fe(100) (Ref. 11) and V(100) are the same to within 50 meV. This indicates that the electronic structure of the  $d$  manifold is not significantly affected by the difference in the structure of the overlayer silver film which occurs as a result of the different lattice parameters of the iron and vanadium substrates.

#### IV. CONCLUSIONS

Using a range of photon energies with high energy and angular resolution, we have studied the development of QW states of  $d$  symmetry in ultrathin silver films (1–5 ML) on a vanadium (100) surface. For a 1 ML film we can identify five  $d$ -band QW states, the full number expected in the absence of spin-orbit coupling. Tight-binding calculations show that the binding energies of the states are, through interaction with the vanadium surface, substantially increased with respect to states in the unsupported silver monolayer. The thickness dependence of the QW-state energies have also been reproduced at least semiquantitatively by the phase accumulation model. The energies of the  $d$ -band QW states in 4 and 5 ML silver films on Fe(100) and V(100) are the same to within 50 meV, indicating that the  $d$ -band dispersion and width are the same despite differences in the structure of the overlayer silver films due to epitaxial strain. Analysis of the width of the leading  $d$ -band QW states has shown that the electrons of  $d$  symmetry in silver films epitaxially grown on V(100) are essentially fully confined within the film, implying a high degree of reflection at the vanadium-silver interface. This shows that the symmetry gap in the substrate is, as a potential barrier, as efficient as a total energy gap.

#### ACKNOWLEDGMENTS

The research work reported in this paper was supported in part by the U.S. Department of Energy under Contract No. DE-ACO2-98CH10886.

<sup>1</sup>D. E. Eastman and W. D. Grobman, Phys. Rev. Lett. **30**, 177 (1973).

<sup>2</sup>B. R. Cooper, Phys. Rev. Lett. **30**, 1316 (1973).

<sup>3</sup>J. G. Tobin, S. W. Robey, L. E. Klebanoff, and D. A. Shirley, Phys. Rev. B **28**, 6169 (1983).

<sup>4</sup>B. T. Jonker, N. C. Bertel, and R. L. Park, J. Vac. Sci. Technol. A **1**, 1062 (1983).

<sup>5</sup>M. Milun, P. Pervan, and D. P. Woodruff, Rep. Prog. Phys. **65**, 99 (2002).

<sup>6</sup>T.-C. Chiang, Surf. Sci. Rep. **39**, 181 (2000).

<sup>7</sup>H. Knoppe and E. Bauer, Phys. Rev. B **48**, 5621 (1993).

<sup>8</sup>A. M. Shikin, O. Rader, G. V. D. Prudnikova, V. K. Adamchuk,

and W. Gudat, Phys. Rev. B **65**, 075403 (2002).

<sup>9</sup>J. Feydt, A. Elbe, H. Engelhard, G. Meister, and A. Goldmann, Surf. Sci. **452**, 33 (2000).

<sup>10</sup>A. M. Shikin, D. V. Vyalikh, G. V. Prudnikova, and V. K. Adamchuk, Surf. Sci. **487**, 135 (2001).

<sup>11</sup>D.-A. Luh, J. J. Paggel, T. Miller, and T.-C. Chiang, Phys. Rev. Lett. **84**, 3410 (2000).

<sup>12</sup>A. Ernst, J. Henk, M. Lüders, Z. Szotek, and W. M. Temmerman, Phys. Rev. B **66**, 165435 (2002).

<sup>13</sup>G. Fuster, J. M. Tyler, N. E. Brener, J. Callaway, and D. Bagayoko, Phys. Rev. B **42**, 7322 (1990).

<sup>14</sup>T. Valla and M. Milun, Surf. Sci. **315**, 81 (1994).

- <sup>15</sup>M. Milun, P. Pervan, B. Gumhalter, and D. P. Woodruff, *Phys. Rev. B* **59**, 5170 (1999).
- <sup>16</sup>K. Meinel, A. Beckmann, M. Klaua, and H. Bethge, *Phys. Status Solidi A* **150**, 521 (1995).
- <sup>17</sup>The possible confusion with respect to the experimentally observed QW peak shifts and the shifts predicted by the phase accumulation formula has been discussed in R. K. Kawakami *et al.*, *Nature (London)* **398**, 132 (1999).
- <sup>18</sup>P. D. Johnson, Y. Chang, and N. B. Brookes, in *Vacuum Ultra Violet Radiation Physics, Proceedings of the 10th VUV Conference*, edited by F. J. Willeumier, Y. Petroff, and I. Nenner (World Scientific, Singapore, 1993); K. Garrison, Y. Chang, and P. D. Johnson, *Phys. Rev. Lett.* **71**, 2801 (1993).
- <sup>19</sup>J. Friedel, P. Lenglar, and G. Leman, *J. Phys. Chem. Solids* **25**, 781 (1964); E. Abate and M. Asdente, *Phys. Rev. B* **140**, B1303 (1965).
- <sup>20</sup>F. Herman and S. Skillman, *Atomic Structure Calculations* (Prentice-Hall, Englewood Cliffs, NJ, 1963).
- <sup>21</sup>Th. Schmitz-Hübsch, K. Oster, J. Radnik, and K. Wandelt, *Phys. Rev. Lett.* **74**, 2595 (1995).
- <sup>22</sup>J. J. Pagel, T. Miller, and T.-C. Chiang, *Science* **283**, 1709 (1999).
- <sup>23</sup>T. Valla and P. D. Johnson (unpublished).
- <sup>24</sup>T. Valla, P. Pervan, and M. Milun, *Vacuum* **46**, 1223 (1995).
- <sup>25</sup>M. Kralj, M. Milun, and P. Pervan (unpublished).
- <sup>26</sup>N. V. Smith, N. B. Brooks, Y. Chang, and P. D. Johnson, *Phys. Rev. B* **49**, 332 (1994).
- <sup>27</sup>S.-Å Lindgren and L. Walldén, *J. Phys.: Condens. Matter* **1**, 2151 (1989).
- <sup>28</sup>D. A. Cleason, S.-Å Lindgren, and L. Walldén, *Phys. Rev. B* **60**, 5217 (1999).
- <sup>29</sup>T. Valla, P. Pervan, M. Milun, and D. P. Woodruff, *Phys. Rev. B* **54**, 11 786 (1996).
- <sup>30</sup>J. J. Paggel, T. Miller, and T.-C. Chiang, *Phys. Rev. B* **61**, 1804 (2000).
- <sup>31</sup>P. M. Echenique and J. B. Pendry, *J. Phys. C* **11**, 2065 (1978).